Overdrive suppression of spontaneously beating chick heart cell aggregates: experiment and theory

ARKADY KUNYSZ, LEON GLASS, AND ALVIN SHRIER
Center for Nonlinear Dynamics, Departments of Physiology and Physics, and Department of Physiology, McGill University, Montreal, Quebec H3G 1Y6, Canada

Kunysz, Arkady, Leon Glass, and Alvin Shrier. Overdrive suppression of spontaneously beating chick heart cell aggregates: experiment and theory. *Am. J. Physiol.* 269 (*Heart Circ. Physiol.* 38): H1153–H1164, 1995.—In spontaneously beating chick heart cell aggregates, sustained periodic stimulation at a rate faster than the intrinsic frequency is generally followed by a transient slowing of the automatic rhythm called "overdrive suppression." We characterize the qualitative aspects of overdrive suppression using three sets of experimental protocols: *1*) stimulation at a fixed frequency with various numbers of stimuli, *2*) stimulation at different frequencies, *3*) stimulation with different intensities. We develop a mathematical model based on a system of nonlinear ordinary differential equations to account for the experimental observations. The main idea of the model is that overdrive suppression arises as a result of a hyperpolarizing current that is induced by action potentials. This work shows that the frequency of action potentials is the major determinant of overdrive suppression. Consequently, during periodic pacing of spontaneous oscillators at different rates, the fastest frequency where 1:1 entrainment can be maintained is associated with maximal overdrive suppression. This type of model is complementary to the development of a rigorous ionic model and can help provide insight into the physiological mechanisms of overdrive suppression.

sinus node recovery test; nonlinear dynamics; mathematical models

SINGLE OR SUSTAINED periodic stimulation can affect the properties of pacemaker cardiac tissue. In particular, rapid stimulation at a rate faster than the intrinsic frequency of the preparation will often lead to a transient slowing of the spontaneous rhythm. This effect is called "overdrive suppression" (25). Overdrive suppression has been observed in cardiac tissues derived from many species (3, 4, 8, 10, 13, 15, 19–21, 24–26). Vassalle (24) demonstrated that an important mechanism underlying overdrive suppression in dog and sheep Purkinje fibers is the activation of an electrogenic Na-K pump. Although subsequent studies confirmed the role of the electrogenic Na-K pump (3, 4, 7, 17, 20, 25), other ionic mechanisms, including extracellular (15, 24) and intracellular calcium accumulation (10, 19), play a role in the overdrive suppression.

Recently, we characterized overdrive suppression in spontaneously beating chick heart cell aggregates (30). We studied the kinetics of buildup and decay of the overdrive suppression after electrical stimulation at constant frequency and demonstrated the role of overdrive suppression in the evolution of rhythms during periodic stimulation. Here, we extend this work by considering the effects of stimulation frequency, amplitude, and duration of pacing on overdrive suppression. Although we are interested in the detailed ionic mechanisms of the heart cell aggregates (14), we believe that development of simplified theoretical models can complement the ionic models by providing easily understandable equations demonstrating the main phenomena. We propose a system of nonlinear ordinary differential equations to model the cardiac oscillator on the basis of the van der Pol equation (6, 23). This oscillator equation is modified by implemention of an additional equation to account for overdrive suppression on the basis of the hypothesis that rapid stimulation induces an electrogenic outward current (24). We assume that each action potential induces an outward current that decays slowly during diastole. At rapid stimulation rates, there is inadequate time between action potentials for the outward current to return to control levels, leading to an increased outward current and lower spontaneous frequency. The outward current plays a role during control activity as well as during electrical stimulation. The experimental results concerning the buildup and decay of overdrive suppression are in good agreement with the simulations of the theoretical model.

MATERIALS AND METHODS

Tissue Culture

Aggregates were prepared using techniques described previously (5, 12). White Leghorn chick embryos were incubated for 7 days at 37°C and 85% relative humidity. They were then decapitated, and their hearts were excised. Atria and ventricles were isolated, fragmented, and then dissociated into single cells in a deoxyribonuclease- and trypsin-containing medium (5). The resulting cell suspension was filtered through a 12.0-μm-diameter-pore-size filter and centrifuged for 15 min at 170 *g*. The cells were resuspended and aliquoted into 25-ml Erlenmeyer flasks containing 3 ml of maintenance medium at densities of 5×10^5–7×10^5 cells/flask. The flasks were then gassed with 5% CO_2-10% O_2-85% N_2, sealed with a silicone rubber stopper, and placed on a gyratory table (70 rpm and 37°C) to allow the formation of spherical aggregates.

The dissociation medium contained 5.25×10^{-5} g/ml crystalline lyophilized trypsin (Worthington Biochemical; 245 U/mg) and 5×10^{-6} g/ml deoxyribonuclease I (Worthington

Biochemical; 9.1×10^4 U/mg) in a Ca^{2+}- and Mg^{2+}-free phosphate-buffered balanced salt solution containing (in mM) 116.0 NaCl, 5.4 KCl, 0.44 NaH_2PO_4, 0.95 $NaHPO_4$, and 5.6 dextrose. A pH of 7.3 was obtained by addition of 1 M HCl or 1 M NaOH.

The maintenance medium contained 20% medium 199 (GIBCO), 4% fetal bovine serum (GIBCO), and 2% horse serum (Kansas City Biological) in a bicarbonate-buffered balanced salt solution. Final concentrations were (approximately, in mM) 116.0 NaCl, 1.3 KCl, 1.8 $CaCl_2$, 0.8 $MgSO_4$, 0.9 NaH_2PO_4, 20.0 $NaHCO_3$, 0.8 $MgSO_4$, and 5.5 dextrose. Gentamicin sulfate (Schering, Garamycin; 10 mg/ml) was added to a final concentration of 5×10^{-5} g/ml.

The enzyme-inactivating medium was similar to the maintenance medium, except for 0% fetal bovine serum, 10% horse serum, and 4 mM KCl (approximately). All solutions were filtered with a 0.22-μm-diameter-pore-size sterile filter.

Electrophysiology

After 48–96 h in culture, the aggregates were transferred to a circular (35 × 10-mm) plastic tissue culture dish (Corning). A thin layer of mineral oil (Klearol, Witco) was poured on top of the medium to prevent evaporation. The bathing medium was gassed from above with 5% CO_2-10% O_2-85% N_2. Temperature was maintained at ~36 ± 1°C. The bicarbonate buffer maintained the medium at a pH of 7.2–7.3. Under such conditions, >95% of the aggregates show spontaneous rhythmic activity. Most of the aggregates studied had a diameter of ~175 μm and contained ~1,500–2,000 cells.

Electrical activity was recorded using borosilicate microelectrodes filled with 3 M KCl (typical microelectrode resistance 40–60 MΩ). Transmembrane potential was recorded, using an amplifier with negative capacitance compensation, to the nearest 0.25 mV. Action potential duration (APD) was measured at 90% repolarization. The bathing medium was kept at virtual ground by coupling to a current-to-voltage converter (10–100 mV/nA) through an agar-salt bridge and a chlorided silver wire. Current pulses were injected into the aggregate via the microelectrode used for recording the transmembrane potential. Currents were measured to the nearest nanoampere. Pulses of current were generated by a microcomputer-based stimulation program (Alembic Software). The duration of the current pulses was 20 ms.

Voltage and injected current waveforms were monitored on a digital oscilloscope (model 5110, Textronix) and recorded on an FM instrumentation recorder (model 3696A, Hewlett-Packard; 3-dB frequency response at 3 impulses/s for direct current to 1,250 Hz) at a tape speed of 3.75 impulses/s for subsequent off-line analysis.

Experiments were carried out in 20 preparations: 15 focused on overdrive at different frequencies and 5 on overdrive suppression for different numbers of stimuli. The electrical activity of the aggregate was recorded in the absence of external stimulation for 5–10 min. Aggregates displaying marked (>5%) variability in the interbeat interval were discarded.

Overdrive suppression for different numbers of stimuli. The aggregates were stimulated with increasing numbers of stimuli. Successive trains of 1, 2, 4, 6, 8, 10, 15, 25, 50, and 100 stimuli, separated by rest periods of ~30 s, were delivered. The period of stimulation was typically ~0.6 T_0 (T_0 is the control cycle length of the preparation), and in all cases there was 1:1 entrainment between the stimulator and the preparation. All measured time intervals were normalized to T_0, which is defined as the average of the five cycle lengths preceding the drive. The postdrive cycle length was evaluated as a function of stimulation duration. The subsequent decay of overdrive was plotted on the same time scale. In some instances, the protocol was repeated for several different amplitudes of stimulation to investigate the relationship between overdrive suppression and the intensity of the stimulus.

Overdrive suppression at different frequencies. Trains of 50 or 100 stimuli were delivered at different stimulation periods (T_s), with a rest of 30 s between successive trains to allow the cycle time to return to control. The period of stimulation was automatically decremented. Different stimulation strengths were also used to investigate the relationship between overdrive suppression and the intensity of the stimulus as well as the entrainment rhythms. The measured time intervals were normalized following the procedure described in the previous protocol.

Data Analysis

Off-line analysis was carried out on the digital oscilloscope and by an automated computer system. Magnetic tapes were played back at 15 impulses/s, and the voltage waveform was sampled at 1 kHz by an IBM-compatible 386 computer through an analog-to-digital interface (Omega). Interbeat intervals were calculated from the digitized waveform by a pattern recognition program (Alembic Software). Computer programs were written to carry out further analysis of the interbeat intervals. Experimental traces were printed on a laser printer (HP Laserjet III) through a graphing package (Grapher).

Theoretical Model

Since the pioneering work of van der Pol and van der Mark (23), simple systems of ordinary differential equations have been used to model qualitative features of biologic oscillators (6, 9, 29). We have chosen a piecewise linear approximation to the van der Pol equations that contains a stable oscillating solution, a limit cycle, to represent the cardiac cycle. For technical details concerning the mathematics, see the APPENDIX.

The theoretical model is designed to capture the important qualitative properties of overdrive suppression in a schematic fashion. The main assumption of this work is that overdrive suppression arises as a consequence of a hyperpolarizing (outward) current that is induced by action potentials. Although we imagine that this current is associated with the transport of positive ions from the intracellular space to the extracellular space during the cycle, we develop the theoretical model in a general way that is consistent with a number of different ionic mechanisms. Therefore the present simplified theoretical model can provide a complementary approach to traditional ionic modeling and represents an important step in our understanding of overdrive suppression.

To carry out this task, the equations for the cardiac oscillator are modified to include a history-dependent hyperpolarizing current. The prolongation of the intrinsic cycle length after rapid stimulation is primarily due to a decrease in the slope of diastolic depolarization and, to a lesser extent, to changes in APD, maximum diastolic potential (MDP), and threshold potential (30).

The differential equations that we adopt for the periodically stimulated cardiac cells are as follows

$$\frac{dV}{dt} = \frac{1}{\epsilon}[y - f(V)]$$

$$\frac{dy}{dt} = \alpha(V) - \beta \frac{Z}{Z + k} \qquad (1)$$

$$\frac{dZ}{dt} = -\gamma \frac{Z}{Z + k} + \Delta Z \delta(t - t_{AP})$$

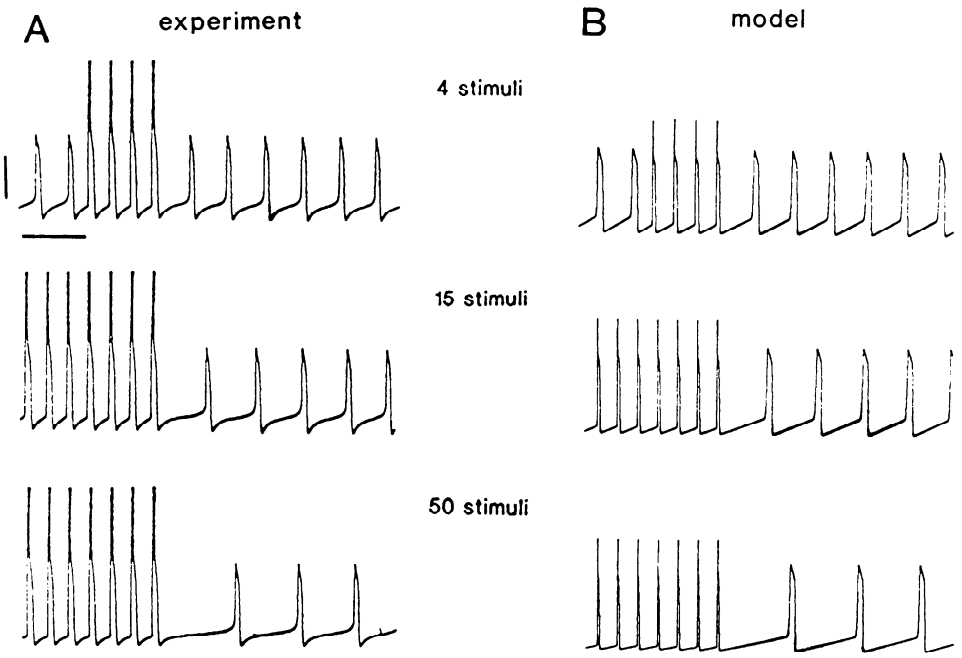

Fig. 1. Traces of membrane voltage showing overdrive suppression after increasing numbers of stimuli of fixed frequency. Stimulation of atrial *aggregate AK71* with a basic cycle length of 470 ms for 4 (*top*), 15 (*middle*), and 50 (*bottom*) stimuli, maintaining a constant stimulation period of 280 ms (0.65 T_0), results in increasing postdrive suppression of automaticity (overdrive suppression). Pulse amplitude was 40 nA; stimulus duration was 20 ms (in all experimental traces). Stimulus artifacts appear as off-scale deflections. *A*: experiments; *B*: simulations. See Table 1 for values of parameters used in this simulation (and for all other protocols and aggregates). Vertical calibration bar, 50 mV; horizontal calibration bar, 1 s. Top of vertical calibration bar indicates zero potential.

where $V(t)$ corresponds to the experimentally observed transmembrane voltage, y controls the timing of the phases of the action potential, and Z is the variable associated with the history-dependent hyperpolarizing current. The properties of the oscillation in the absence of Z are determined by the piecewise linear functions $f(V)$ and $\alpha(V)$ (see APPENDIX). Finally, ϵ, β, γ, and ΔZ are positive constants, δ is the Dirac delta function,[1] and t_{AP} represents the time of upstroke of the action potential.

The physical interpretation of *Eq. 1* is as follows. If we first fix $Z = 0$, there will be a stable oscillation of V and y. For $0 < \epsilon \ll 1$, the oscillation is similar to a cardiac action potential with periodic rapid increases in V that we associate with the successive onsets of the action potential. Now consider what happens when Z is allowed to vary. The onset of the action potential leads to an instantaneous increment, ΔZ, of the factor Z. Meanwhile, during the entire cycle, the level of Z is reduced following some Z-dependent rate. There is an associated term, $-\beta[Z/(Z + k)]$, influencing the dynamics of y in the second equation. This term prolongs the duration of the depolarizing (pacemaker) phase of the cardiac cycle and, to a lesser extent, decreases the duration of the plateau of the action potential. Therefore the removal of Z can be associated with a hyperpolarizing current, where the magnitude of the current is proportional to $Z/(Z + k)$ (see APPENDIX).

Numerical simulations were carried out by integrating *Eq. 1* with use of a fourth-order Runge-Kutta method. To eliminate transients, initial conditions were chosen to lie on the limit cycle. The parameters of *Eq. 1* were adjusted for each aggregate studied with use of the method described in the APPENDIX.

RESULTS

Overdrive Suppression at Fixed Stimulation Frequency for Different Numbers of Stimuli and Different Stimulus Intensities

In this protocol, the aggregates were stimulated for several different durations, maintaining a constant stimulation frequency. Figure 1*A* shows a typical experiment from an aggregate with $T_0 = 520$ ms stimulated at a stimulation period of 300 ms ($\sim 0.58\ T_0$). Initiation of the drive is generally followed by a transient depolarization, which may reflect changes in ionic gradients across the membrane. A hyperpolarization (increase in MDP) can sometimes be observed during the longer (1 min at 3 Hz) drives in spontaneously beating embryonic chick heart cell aggregates (20) but was not clearly present in our experiments. After 4, 15, and 50 stimuli, the first interbeat interval after the drive, T', was prolonged by 20, 70, and 160%, respectively, over control.

The results of periodic stimulation for the same number of stimuli and the same stimulus periods in the theoretical model are shown in Fig. 1*B*. The degree of postdrive suppression of activity is roughly comparable to that in the experimental system. However, because the time-dependent process described in *Eq. 1* does not influence the geometry of the limit cycle, no drive-induced hyperpolarization in MDP is found in the theoretical results (see APPENDIX).

Figure 2 illustrates how overdrive suppression is induced in the theoretical model during periodic stimulation (1, 4, and 15 stimuli) at a rate faster than control. The *top traces* show $V(t)$; the corresponding changes in the level of Z are presented in the *bottom traces*. The control cycle length is 500 ms, and the stimulus period is 300 ms. The upstroke phase of the action potential is associated with a significant increase ($\sim 30\%$) in the level of Z. Under control conditions (before stimulation), the same quantity of cations Z is removed by the electrogenic mechanism active during the entire cycle. During periodic stimulation, increased action potential frequency results in accumulation of Z, which stimulates the electrogenic mechanism, hence reducing the slope of diastolic depolarization. As in Fig. 1, the apparent decrease in APD during overdive in the model is due to the geometry of the limit cycle (see APPENDIX). After cessation of stimulation, the level of Z decays because of

[1] The Dirac delta function $\delta(s - s_0)$ is defined by its assigned properties: $\delta(s - s_0) = 0$ for any $s \neq s_0$ and $\int_{-\infty}^{\infty} ds f(s)\delta(s - s_0) = f(s_0)$ for any function f continuous in the argument s.

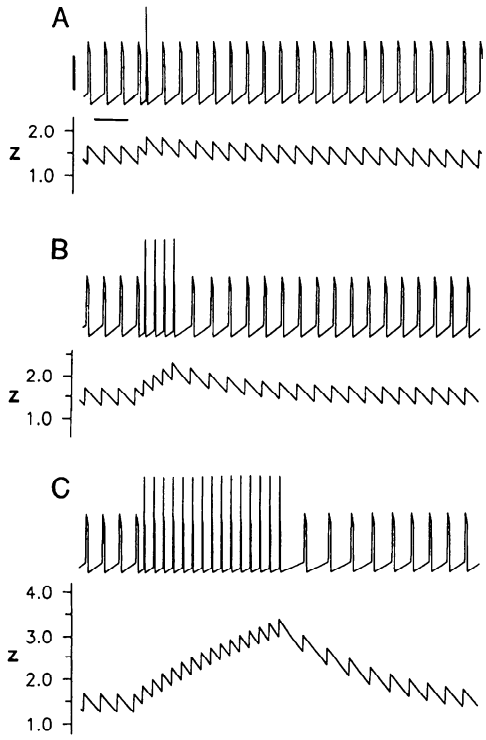

Fig. 2. Numerical simulations of model showing relationship between overdrive suppression and level of Z. Parameters in model were adjusted to obtain control cycle length of 500 ms. Trains of 1, 4, and 15 stimuli (A, B, and C, respectively; T_s = 300 ms) were applied (1:1 entrainment), and resulting traces for $V(t)$ and $Z(t)$ (in units of k) are presented. Under control conditions, level of Z varies by ~30% within cycle. Overdrive suppression is due to increased magnitude of Z-sensitive electrogenic current, because high action potential frequency during periodic stimulation causes accumulation of Z. This overdrive suppression decays subsequently, and within 10–15 s control activity is restored. Calibration bars as in Fig. 1.

the increased extrusion via the hyperpolarizing current and the slowing of spontaneous activity (overdrive suppression). After 15 stimuli, the twofold increase in the level of Z is associated with a 50% increase in the cycle length. Six seconds after cessation of stimulation, the level of Z is only 10% above normal and control activity has almost resumed.

A composite of overdrive suppression, expressed as T'/T_0 vs. stimulation time, is shown in Fig. 3 for two different atrial aggregates stimulated with T_s = 300 and T_s = 310 ms. The postdrive pause developed slowly with the number of stimuli applied. As the number of stimuli applied increased further, the postdrive prolongation sometimes showed a tendency to saturate (30). Fig. 3B shows the results of simulation. There is good agreement between the numerical simulation and experimental data concerning the magnitude of the overdrive effect and its dependence on the number of stimuli applied. In the numerical simulation, however, the decay rate of overdrive suppression is initially too slow and then becomes too fast.

During sustained periodic stimulation at a fixed frequency, the observed entrainment pattern is often a function of the stimulus intensity (11, 12, 14, 30). For example, as the amplitude of the stimulus is varied while the period of stimulation is maintained constant, different types of N:M locking between the stimulator and the preparation can be observed. The traces in Fig. 4 were obtained by maintaining a constant period of stimulation (T_s = 145 ms), but with stimulation intensities of ~18 nA in A, ~28 nA in B, and ~40 nA in C. As the stimulation intensity increases, there are different coupling patterns between the stimulus and the aggregate with 2:1 locking in A, 3:2 locking in B, and 1:1 locking in

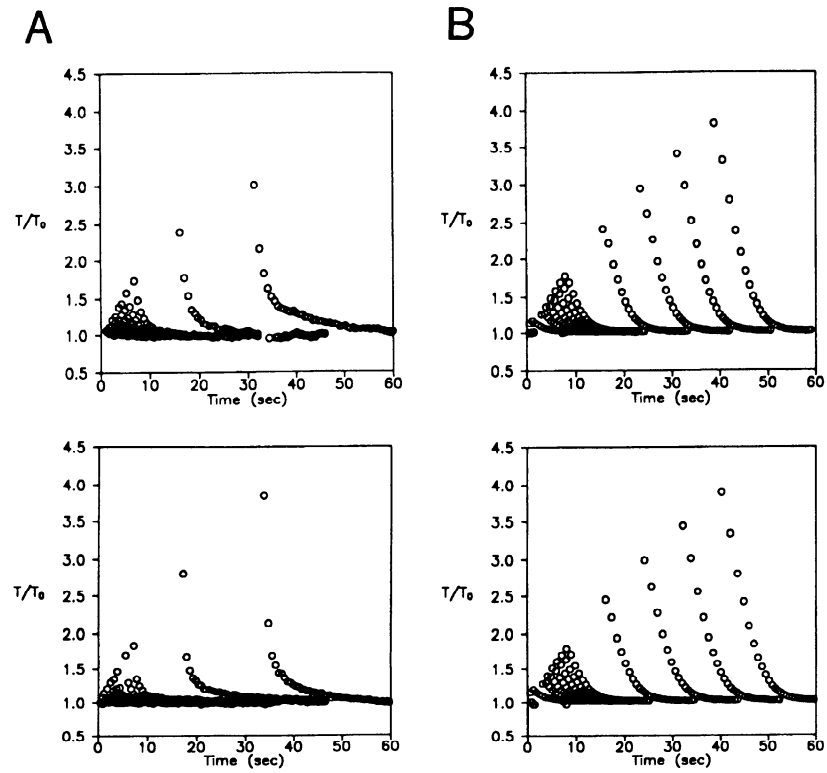

Fig. 3. Composite of overdrive suppression as a function of stimulation time for atrial *aggregates AK61* and *AK71* stimulated with T_s = 310 ms and T_s = 300 ms, respectively. Interbeat intervals after drive, normalized to control cycle length (T'/T_0), are shown for increasing stimulus train durations. After drive, 1st cycle length is the longest, and normal activity is restored after 10–30 s. A: experiments; B: model simulations.

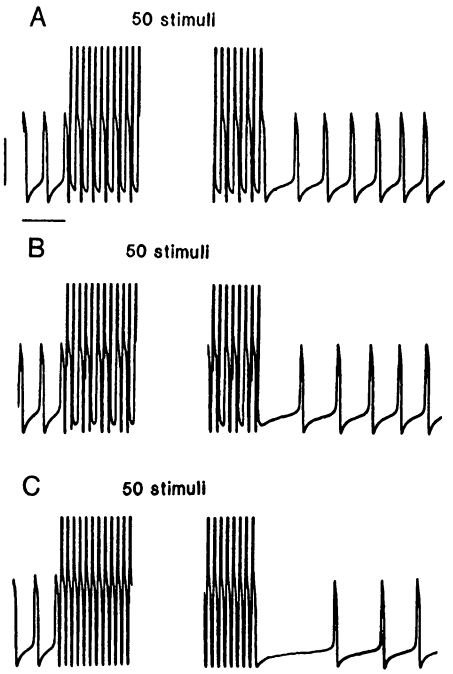

Fig. 4. Recordings showing dependence of overdrive suppression on action potential frequency. A 180-μm-diam atrial aggregate with control cycle length of 470 ms (*aggregate AK71*) was stimulated with trains of 50 pulses of fixed period (T_s = 145 ms) but different stimulus intensities. *A*: 2:1 locking, pulse amplitude ~18 nA; *B*: 3:2 locking, stimulus intensity ~28 nA; *C*: 1:1 locking, stimulus amplitude ~40 nA. For a fixed rate of pacing, overdrive suppression is directly proportional to action potential frequency. For clarity, not all pulses are shown. Calibration bars as in Fig. 1.

C. The changes in the locking ratio are associated with changes in the overdrive suppression. After stimulation leading to 1:1 phase locking, the postdrive prolongation reached 340% over control, but this was reduced to 120% over control after 3:2 locking and to 70% over control after 2:1 locking. Similar results were obtained in six other preparations. This demonstrates that it is the frequency of the action potentials, rather than the period of stimulation, that is most critical in determining the magnitude of the overdrive suppression.

Overdrive Suppression at Different Frequencies

During periodic stimulation, different coupling rhythms between the stimulus and the preparation can be observed by changing stimulation intensity or stimulation frequency (11, 12, 14, 30). In the range of 1:1 entrainment during periodic stimulation with $T_s < T_0$, there is overdrive suppression, where the increase in the magnitude of the slowing of the intrinsic rate is inversely proportional to T_s. This is illustrated in Fig. 5, which shows three traces recorded from a 180-μm 7-day-old atrial aggregate with T_0 = 520 ms. The aggregate was subjected to 50 stimuli for 145, 250, and 355 ms. In all three cases, there was stable 1:1 entrainment between the stimulator and the aggregate. After the drive, the first interbeat interval was prolonged by 300, 140, and 40%, respectively over control. Thus the postdrive prolongation after a fixed number of stimuli increases as the period of stimulation decreases, provided there is a maintained constant rhythm.

An interesting property of the experimental preparation is that it can be entrained in 1:1 fashion to periodic depolarizing stimuli with $T_s > T_0$. However, this effect is much more difficult to observe than the 1:1 entrainment with $T_s < T_0$ and could be measured in four preparations only (Fig. 6). In these cases, after cessation of stimulation, the intrinsic rate is slightly elevated, an effect that has been called underdrive acceleration (25). The importance of this effect is that it indicates a contribution of an electrogenic hyperpolarizing current, even during control conditions, which is consistent with the theoretical model.

As the stimulation frequency increases, maintaining the stimulation intensity fixed, there is typically a critical stimulation frequency that sets the fastest rate at which 1:1 entrainment can be maintained (11, 14, 30). In the 1:1 entrainment zone, the length of the first beat after the drive is inversely proportional to the period of pacing. At faster stimulation frequencies, there are *N:M* rhythms with $N > M$, as in Fig. 4, where the magnitude of the overdrive effect decreases as a consequence of the dropped beats. In all the preparations studied, this "peaking" phenomenon was related to sudden changes in action potential frequency resulting from the transition from *N:M* to *N′:M′* phase locking with $N'/M' \geq N/M$. This is illustrated in Fig. 7, *A* and *B*, which shows the duration of the first beat after overdrive stimulation in a single aggregate at two stimulation intensities for

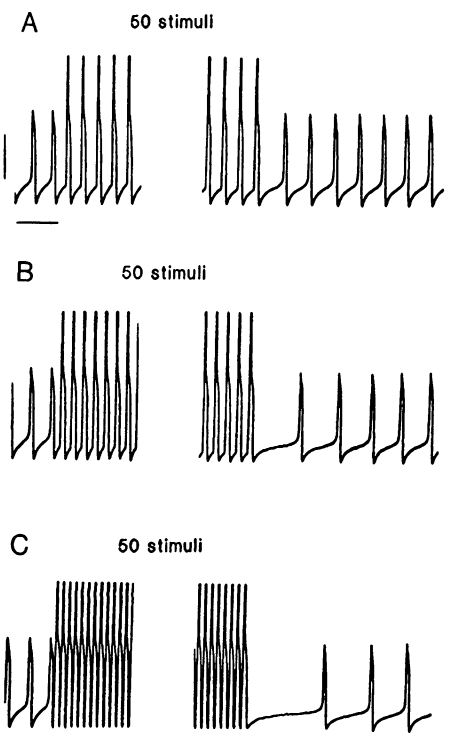

Fig. 5. Traces from 180-μm 7-day-old atrial aggregate with control cycle length of 470 ms (*AK71*, same as in Fig. 6). Aggregate was stimulated for 50 stimuli at 355 (*A*), 250 (*B*), and 145 ms (*C*), during which 1:1 locking was maintained. Pulse amplitude was fixed at ~40 nA. Postdrive prolongation increases with shorter periods of stimulation (higher action potential frequencies). Calibration bars as in Fig. 1.

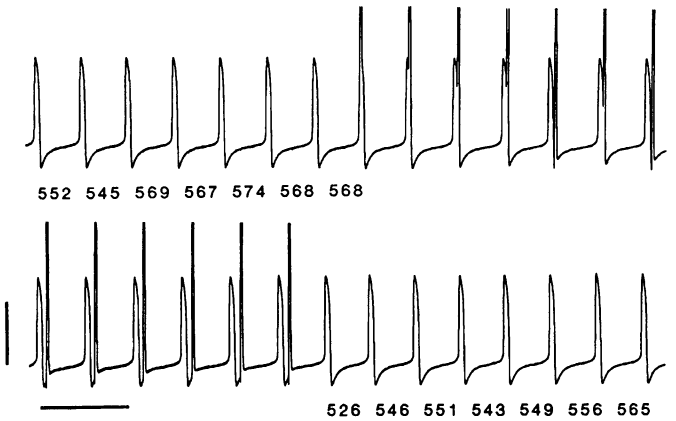

Fig. 6. Periodic stimulation at a rate slower than intrinsic rate but maintaining 1:1 locking in 150-μm atrial aggregate (*AK61*) with control cycle length of 560 ms. *Top trace:* sample of control activity before stimulation. *Bottom trace:* aggregate stimulated in a 1:1 fashion with ~20-nA pulses. Timing of pulses is indicated by off-scale vertical deflections. Stimulation period was 580 ms. Length of successive interbeat intervals (in ms) after pulse train is indicated below experimental trace. After termination of stimulation, there is a slight acceleration of intrinsic rhythm, or underdrive acceleration (~6%), with a slow recovery to control. This effect shows that electrogenic mechanism is active, even under control conditions, which is in agreement with theoretical model. Calibration bars as in Fig. 1.

50 stimuli. At the higher stimulation intensity (Fig. 7, *A* and *B, right*), the 1:1 entrainment was maintained for shorter stimulation periods ($T_s/T_0 = 0.3$), whereas with the weaker stimulation intensity (Fig. 7, *A* and *B, left*), the 1:1 entrainment was maintained until $T_s/T_0 = 0.45$. Figure 7*C* shows data in the same format superimposed for six different aggregates, including Fig. 7, *A* and *B*, with use of different stimulus amplitudes. For each aggregate, the postdrive prolongation and the period of stimulation have been normalized to the respective T_0. For stimulation periods where 1:1 entrainment was found for all six aggregates, overdrive suppression, scaled to the intrinsic cycle length, was approximately the same, independent of the preparation and the stimulus strength.

Figure 8 is a composite of the first postoverdrive cycle length after 50 stimuli as a function of the period of the stimulation for five different aggregates superimposed on the theoretical simulation. The measured time intervals are normalized to T_0. The parameters used in the numerical simulation were set for each aggregate according to the procedure described in the APPENDIX. The values used in the numerical simulation are presented in Table 1. In all five aggregates, there is a similar dependence of overdrive suppression on the period of stimulation (scaled to intrinsic cycle length). This behavior is consistent with the numerical simulation of the theoretical model.

DISCUSSION

We have documented the effects of stimulation history on the overdrive suppression of spontaneous activity of chick atrial heart cell aggregates. The magnitude of overdrive suppression is, for a given entrainment pattern, proportional to the duration of the stimulation and inversely proportional to the period of stimulation. These findings are consistent with previous observations in chick heart cell aggregates (20, 30) as well as studies in a number of different preparations, including

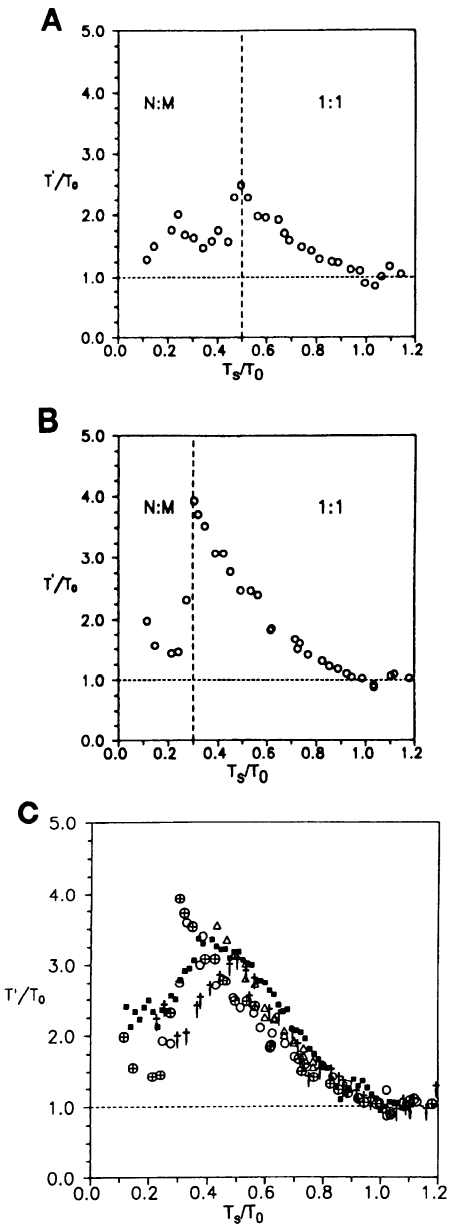

Fig. 7. Duration of 1st beat after overdrive stimulation in a single aggregate (*A* and *B*, *aggregate AK71*) at 2 different stimulation intensities for 50 stimuli and for 5 different aggregates (*C*) as a function of stimulus period. In *A* and *B*, at higher stimulation intensity (*right*), 1:1 entrainment was maintained for shorter stimulation periods ($T_s/T_0 = 0.3$), whereas with weaker stimulation intensity (*A*), 1:1 entrainment was maintained until $T_s/T_0 = 0.45$. *C*: composition of data from *aggregates AK34* (+), *AK36* (■), *AK70* (△), *AK71* (●), and *AK78* (□), with postdrive prolongation and period of stimulation normalized to respective control cycle lengths. In 1:1 entrainment region, magnitude of overdrive suppression is not a function of amplitude of stimulation and is approximately the same for all preparations. Decrease in overdrive suppression observed at high stimulation frequencies corresponds to increasing degrees of block (lower action potential frequency) during stimulation.

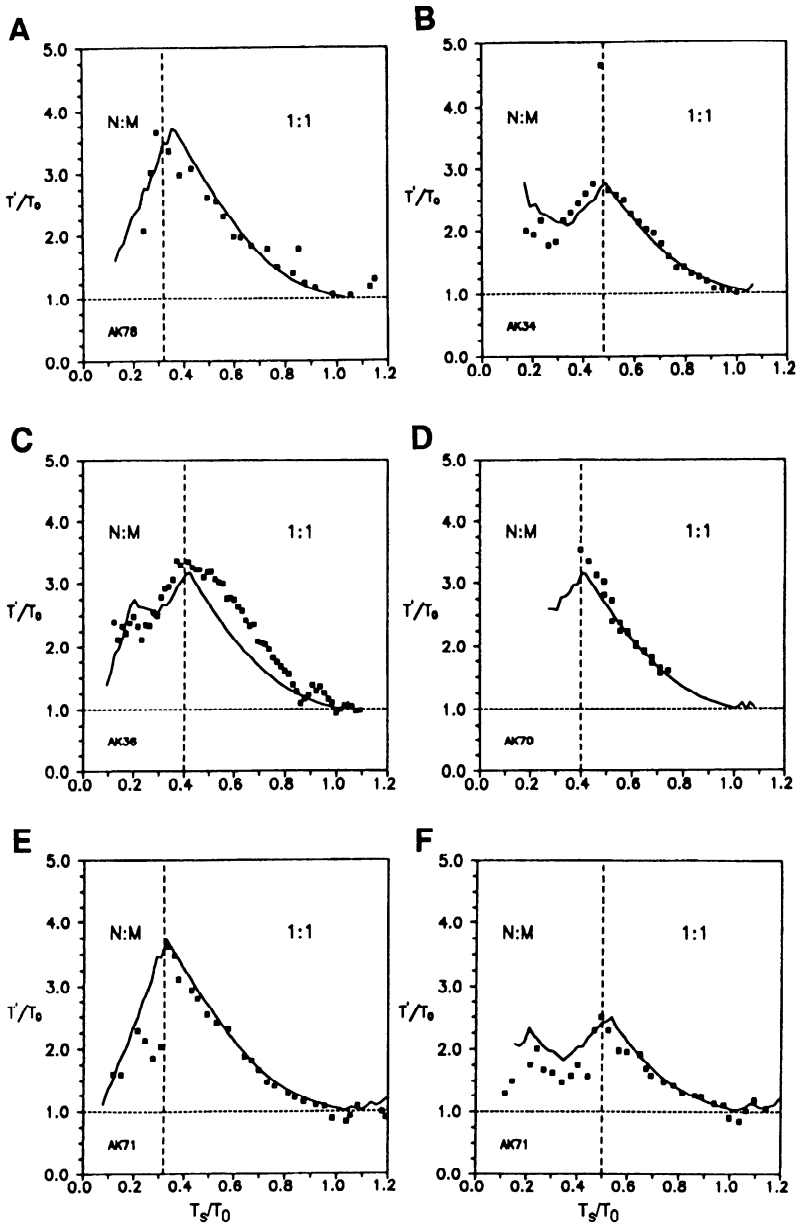

Fig. 8. Composite of 1st cycle length after 50 stimuli as a function of period of stimulation for 5 different aggregates (filled symbols) superimposed on theoretical stimulation (solid line). Data in *E* and *F* were obtained from the same aggregate with use of 2 different stimulus amplitudes. See Table 1 for values of parameters used in simulations for each aggregate (*AK78, AK34, AK36, AK70, AK71*).

Table 1. *Summary of parameters used in numerical simulations*

Aggregate	T_0, APD, ms	$T'(\phi = 0.5)/T_0$	α_4, α_{APD}, s^{-1}	ΔZ, k	γ, k/s	Stimulation Amplitude, mV
AK71	520, 80	1.07	5.68, 9.09	0.41	1.33	90 and 100
AK78	620, 85	1.08	4.67, 8.96	0.46	1.25	100
AK70	620, 100	1.07	4.81, 7.11	0.42	1.12	97
AK34	470, 65	1.07	6.17, 11.68	0.41	1.44	93
AK36	640, 100	1.07	4.63, 7.22	0.41	1.08	97
AK61	540, 80	1.07	5.43, 9.24	0.41	1.27	120

T_0, control cycle length; APD, action potential duration; T', 1st interbeat interval after drive; α_4 and α_{APD}, positive constants related to duration of phase 4 and APD, respectively; ΔZ and γ, positive constants; k, parameter that sets scale of Z (variable associated with history-dependent hyperpolarizing current).

Purkinje fibers in sheep (24, 25) and dogs (8, 24, 25) and sinoatrial node in rabbits (19, 21), guinea pigs (10), and humans (13). In chick heart cell aggregates and other preparations, very fast pacing may lead to a partial block of activity (11, 30). Under such circumstances, for a fixed number of stimuli, overdrive suppression decreases with increasing degree of block (i.e., lower action potential frequency). This is in agreement with the idea that the frequency of action potentials is the major determinant of the postdrive prolongation in the cycle length (24, 25).

The development of the theoretical model was motivated by a desire to present a relatively clear mathematical picture based on physiologically plausible assumptions and in reasonable agreement with qualitative experimental evidence. Our formulation offers several advantages: *1*) the model is based on a two-dimensional

approximation to the cardiac oscillator, which is not preparation specific and may therefore be applicable to a wide class of biologic systems; and *2*) this comparatively simple model can represent a useful step toward the integration of an overdrive-inducing mechanism in a high-dimensional ionic model, because it captures most of the qualitative aspects of overdrive suppression in this preparation.

Overdrive suppression has been related to several mechanisms, such as the stimulation of the Na-K pump via an increased level of internal sodium (3, 4, 7, 17, 20, 24, 25), accumulation of potassium outside the cells (15, 24), augmented uptake of calcium (10, 19), and release of neuromediators (27). In embryonic chick heart cells, overdrive suppression was found to be reduced by ouabain, an extracellular blocker of the Na-K pump (17, 20). Because the Na-K pump plays a major role in overdrive suppression in chick heart cell aggregates, it is tempting to believe that, for this preparation, the theoretical model is a crude approximation to the mechanisms underlying the influx (fast sodium current) and the active transport (sodium pump) of sodium ions.

A connection can be made between the model and the induction of overdrive suppression by assuming that the influx of cations Z into the cell during the upstroke phase of the action potential represents the influx of sodium ions. To maintain a constant beat-to-beat level of intracellular Z, this same quantity of ions Z is extruded via some Z-sensitive (Michaelis-Menten kinetics) electrogenic mechanism active during the entire cycle. Increased entry of cations Z during fast pacing (higher action potential frequency) activates the electrogenic mechanism, which in turn slows diastolic depolarization, transiently suppressing automatic activity. After the drive, the intracellular level of Z is gradually restored and the cycle length returns to control. After a fixed number of stimuli, the postdrive prolongation is longer for faster stimulation rates. Thus the theoretical model is consistent with a body of experimental results that has accumulated over the past 25 years (13, 24, 25).

To be able to account for the overdrive suppression following a single premature action potential, we must assume a very significant variation ($\leq 30\%$) in the level of Z during the cycle. The present theoretical model does not incorporate any assumptions concerning the structure and the geometry of the intracellular space. Consequently, one may suppose that the large changes in the level of Z remain confined to a partition of the intracellular space that is available to the Z-sensitive electrogenic mechanism. In fact, to properly describe the Na/Ca exchange in excitable cells, several authors suggest a hypothetical compartmentalization of the intracellular space available to incoming sodium ions (2, 16). Although the existence of this "fuzzy space" remains unproven, it offers a possible explanation for the large changes in the level of Z we must assume in the theoretical model.

These considerations should be useful in developing a detailed ionic model for this system. This type of model is needed to overcome some of the limitations of the current model. For example, this simplified model does not adequately reproduce the experimentally observed APD or phase-resetting behavior. There is shortening of the APD during overdrive in the experiment and in the model (Fig. 1). In the model, the APD is shortened when a strong stimulus is applied early during phase 4, causing the trajectory to join the downward branch of the limit cycle toward the end of the action potential (see APPENDIX). In the real system, the APD depends on complex interactions between inward and outward currents. Similarly, as discussed in detail elsewhere (14), accurately reproducing experimentally observed phase resetting is a difficult challenge but one that must be confronted by accurate ionic models.

The current theoretical model allows one to predict other types of kinetic behaviors that might arise from changes in parameters. Previous studies have found that the magnitude of the overdrive suppression saturates after prolonged stimulation (10, 24). However, in our theoretical model, whether or not the overdrive suppression saturates depends on the parameters for the kinetics of the inflow and extrusion of Z as well as the frequency of stimulation. When very-high-frequency stimulation is applied, the influx of cations Z may exceed the extrusion capacity of the fully activated electrogenic mechanism. Under these conditions, provided that 1:1 entrainment can be maintained, the theoretical model predicts that postdrive prolongation would not saturate and that there could be very long prolongations until activity resumed. This could be of potential clinical relevance in the setting of prolonged supraventricular tachycardia.

The current study may have implications in the study of rhythms observed in other systems. For example, sustained periodic stimulation at fast frequencies may induce "fatigue" in the atrioventricular node (1) and changes in the Purkinje fiber conduction properties (8), sometimes leading to a complex evolution of rhythms (22). In patients undergoing the sinus node recovery test, an unusually long postdrive suppression of activity is often associated with sick sinus syndrome (13). During this clinical test, as the frequency of the stimulation is increased, the postdrive pause reaches a maximum and then diminishes (13). The present study suggests that this peaking phenomenon may be related to changes in action potential frequency during periodic stimulation. However, the actual mechanisms responsible for overdrive suppression in the sinoatrial node may be very different from those in the atrial aggregates, and there may be rate-dependent contributions from changes in neurohumoral factors (27) as well as changes in sinoatrial conduction during overdrive.

We have demonstrated time-dependent effects of stimulation on the cycle length of spontaneously beating atrial chick embryo aggregates. This study reports the first extensive experimental and theoretical investigation of frequency-related qualitative changes in the intrinsic cycle length after overdrive in embryonic chick atrial heart cell aggregates. Our theoretical approach is based on a system of ordinary differential equations, and the hypothesis that overdrive suppression in this preparation is due to the activation of a hyperpolarizing

current via an increased action potential frequency has been used with reasonable success to reproduce the qualitative aspects of overdrive suppression observed experimentally. The results here should be useful in the development of more rigorous ionic models of the mechanisms of overdrive suppression.

APPENDIX

Theoretical Model

We provide technical details on the properties of the differential equation used to model the cardiac oscillator. The two-dimensional system of ordinary differential equations that is used to model the action potential in the absence of the hyperpolarizing current is based on a modified version of the van der Pol equation (6, 23) as follows

$$\frac{dV}{dt} = \frac{1}{\epsilon}[y - f(V)]$$
$$\frac{dy}{dt} = \alpha(V) \qquad (A1)$$

where $f(V)$ and $\alpha(V)$ are piecewise linear functions of V and ϵ is a positive constant. For $0 < \epsilon \ll 1$, *Eq. A1* is taken as a prototypical example of a limit cycle oscillation with fast relaxation to the limit cycle. The parameters and functions in *Eq. A1* were selected so that $V(t)$ corresponds roughly to the experimentally observed transmembrane voltage. For the heart cell aggregates, we assume that

$$f(V) = \begin{cases} \dfrac{V}{20} + 4, & V \le -60 \\ -\dfrac{V}{80} + \dfrac{1}{4}, & -60 < V < 20 \\ \dfrac{V}{20} - 1, & V \ge 20 \end{cases}$$

and α is a piecewise constant function of V, such that

$$\alpha(V) = \begin{cases} \alpha_4, & V < 0 \\ -\alpha_{APD}, & V \ge 0 \end{cases}$$

where α_4 and α_{APD} are positive constants related to the duration of phase 4 (diastolic depolarization) and APD, respectively (see below).

A representation of the limit cycle in the $V - y$ plane (phase plane) is shown in Fig. 9*A*. The phase plane is divided into several regions corresponding to the phases of the cardiac cycle: the upstroke (*region I*), the plateau of the action potential (*region II*), the repolarization (*region III*), and the diastolic depolarization (*region IV*). The solid line represents the V nullcline, i.e., the set of points such that $dV/dt = 0$. The dotted line shows the trajectory of a phase point as it travels on the limit cycle. Provided $0 < \epsilon \ll 1$ (we will assume in what follows that $\epsilon = 25{,}000^{-1}$), the cycle can be divided into two phases: the action potential and *phase 4*. The durations of the action potential, t_{APD}, and *phase 4*, t_4, and can be found by direct integration of *Eq. A1*. The duration of *phase 4* is the length of time for y to increase from 0 to 1. Because $dy/dt = 1/\alpha_4$ during *phase 4*, we immediately find

$$t_4 = \frac{1}{\alpha_4}$$

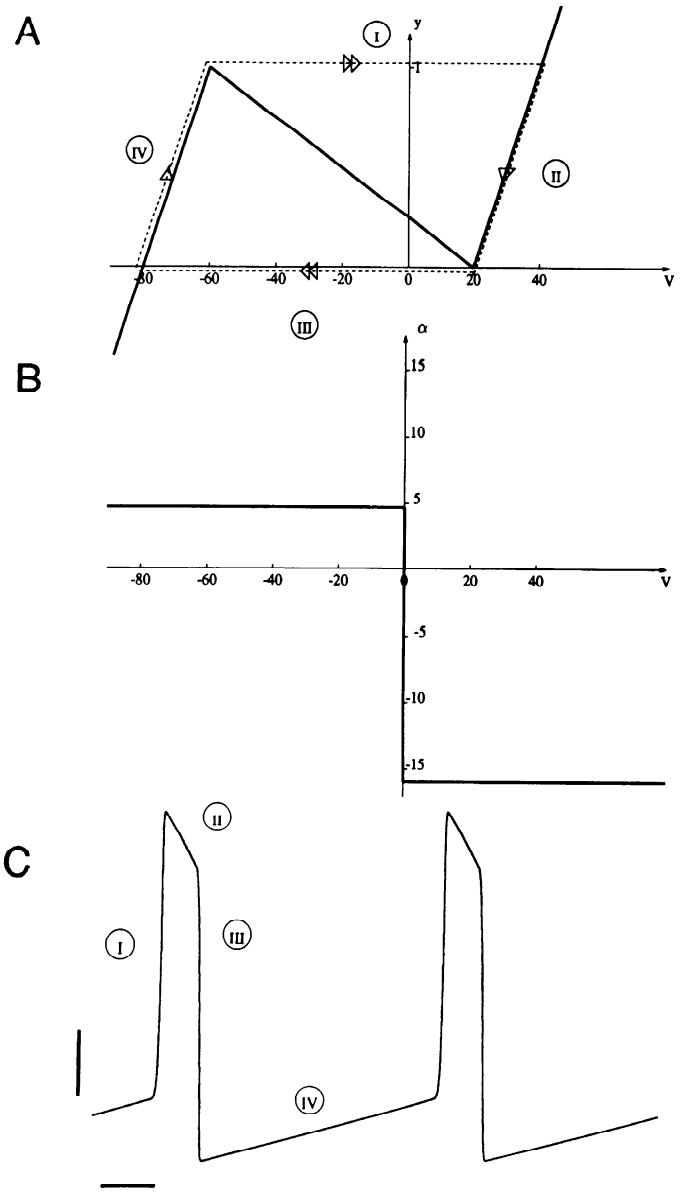

Fig. 9. Geometry of functions $f(V)$ and $\alpha(V)$ in *Eq. A2* with assumption that Z is fixed at 0 and $\epsilon \ll 1$. *A*: $V - y$ phase plane. Solid line, nullcline (i.e., set of points such that $dV/dt = 0$), corresponding to function $f(V)$; dashed line, approximate sketch of limit cycle, with various regions associated with phases of action potential. *B*: geometrical representation of discontinuous function $\alpha(V)$. In *regions II* and *IV* of phase plane, value of $\alpha(V)$ is directly proportional to dV/dt. *C*: result of corresponding simulation of $V(t)$. Different phases of action potential are indicated. Horizontal calibration bar, 100 ms; vertical calibration bar, 20 mV.

Similarly

$$t_{APD} = \frac{1}{\alpha_{APD}}$$

The relationship between α_4, α_{APD}, and V is summarized in Fig. 9*B*. An example of an action potential generated by this equation is shown in Fig. 9*C*. In numerical simulations, the model is driven by periodically adding a positive (depolarizing stimulus) constant to V. Because the limit cycle is strongly attracting, high-amplitude stimulation at an early phase of the cycle may elicit a premature action potential with shortened duration (see Figs. 1 and 2). Although this is inconsistent with

experimentally measured behavior, changes in APD play a negligible role in overdrive suppression in this preparation (30).

In the presence of the hyperpolarizing current associated with Z, the dynamics are given by *Eq. 1*, which is repeated here, with the substitution $g(Z) = Z/(Z + k)$

$$\frac{dV}{dt} = \frac{1}{\epsilon}[y - f(V)]$$

$$\frac{dy}{dt} = \alpha(V) - \beta g(Z) \qquad (A2)$$

$$\frac{dZ}{dt} = -\gamma g(Z) + \Delta Z \delta(t - t_{AP})$$

where β, γ, and ΔZ are positive constants and t_{AP} is the time of the onset of the action potential. We assume that the removal of Z follows Michaelis-Menten kinetics, so that $g(Z) = Z/(Z + k)$, where k is a parameter that sets the scale of Z. As before, simulation of stimulation is carried out by adding a positive (depolarizing) constant V. We associate the start of the action potential with the time when the trajectory crosses the line $f(V) = -V/80 + 1/4$ while V increases.

Analysis of the Theoretical Model

For each aggregate, it is necessary to specify six parameters: α_4, α_{APD}, β, γ, ΔZ, and k. We briefly give our strategy for determining the values of these parameters and then give the details.

One of the experimental findings is that the slope of *phase 4* after overdrive suppression may be quite small but is never negative. In the context of the theoretical model, this means that $\beta = \alpha_4$, so that with maximum overdrive the slope of *phase 4* approaches 0. The parameter k is used to set the scale of Z, so it is arbitrary. In the computations, we will express the concentrations of Z in units of k. The parameters α_4 and α_{APD} are related to the duration of *phase 4* and the APD, respectively, with use of relations we give below, and are computed from measured values of these phases of the action potential appropriately modified by the effects of the overdrive term under control conditions. This leaves only two parameters, γ and ΔZ. We derive expressions that relate these two parameters to T_0, the cycle length that is found after a cycle induced by a stimulus delivered at phase ϕ during *phase 4* [$T'(\phi)$], and the mean value of Z during a control cycle ($\overline{Z}_0$).

For the computations that follow, in which it is necessary to compute the duration of various phases of the cycle, it is convenient to approximate the function $g(Z)$ by its mean value during a cycle. The justification for this approximation is based on the power series expansion around the mean value $\overline{Z}$ during the cycle. We find that

$$g(Z) = \frac{\overline{Z}}{\overline{Z} + k} + \frac{k}{(\overline{Z} + k)^2}(Z - \overline{Z}) + \cdots$$

Comparison of the magnitudes of the first terms shows that the first-order term is ≥ 10 times smaller than the zeroth-order term as long as $|Z - \overline{Z}|$ is $< 0.4k$. Under control conditions or after a single premature action potential, the changes in the level of Z are at most of the order of $0.5k$ for all the aggregates studied (Table 1, Fig. 2). During the cycle, we can therefore approximate the function $g[Z(t)]$ by

$$g(\overline{Z}) = \frac{\overline{Z}}{\overline{Z} + k} \qquad (A3)$$

The duration of *phase 4* (diastolic depolarization), t_4, can be calculated from the above equations. The duration of *phase 4* is determined by the integral

$$1 = \int_0^{t_4} dy = \int_0^{t_4} ds\{\alpha_4 - \alpha_4 g[Z(s)]\}$$

Because at the end of *phase 4* we have $y(t) = 1$, the duration of *phase 4* can be approximated

$$t_4 = \frac{1}{\alpha_4 - \alpha_4 g(\overline{Z})} \qquad (A4)$$

A similar expression can also be obtained for the APD

$$APD = \frac{1}{\alpha_{APD} + \alpha_4 g(\overline{Z})} \qquad (A5)$$

The expressions for the effects of overdrive stimulation of the heart cell aggregates are in qualitative agreement with experimental observations: the duration of *phase 4* increases while APD decreases. However, because α_{APD} is approximately twice the magnitude of α_4 (Table 1), the effect of overdrive on APD (after the drive) is small compared with the effect on the duration of *phase 4*. Consequently, to facilitate computations, in the estimation of parameters we will assume that APD is constant, so that, under control conditions, the cycle length is

$$T_0 = APD + \frac{1}{\alpha_4 - \alpha_4 g(\overline{Z}_0)} \qquad (A6)$$

We now consider the effect of a single stimulus on the cycle length delivered at a phase ϕ during *phase 4* of a control cycle that induces an action potential. The period of the cycle after the stimulus is T', and the mean value of Z during the cycle is $\overline{Z}$. Because the resulting perturbation in the cycle length is small (experimentally measured: ~7% on average for $\phi = 0.5$),

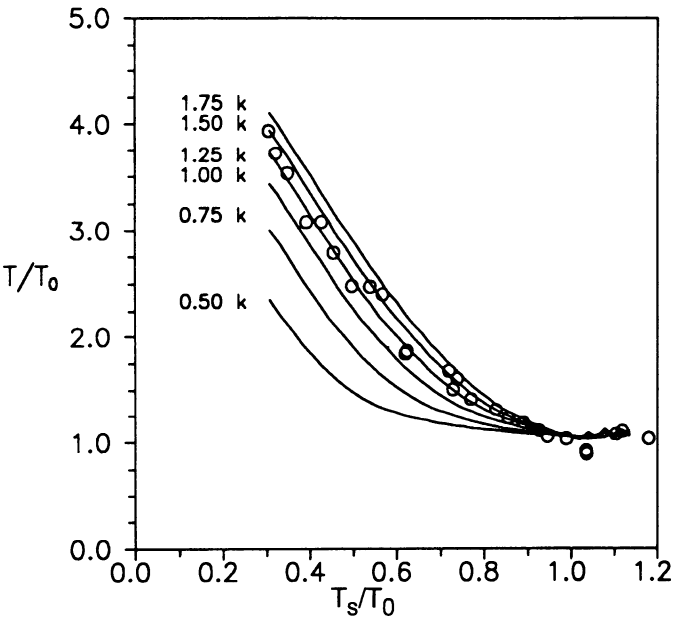

Fig. 10. Procedure to determine value of $\overline{Z}_0$ (average control level of Z). ○, Typical experimental data for overdrive suppression at different periods of stimulation (*aggregate AK71*) normalized to control cycle length. Solid lines, results of corresponding simulation with use of 6 different values of $\overline{Z}_0$ (as indicated at *left* in units of k). For $\overline{Z}_0$ between $1.25k$ and $1.75k$, there is good agreement with experimental data. Average value of $\overline{Z}_0 = 1.50k$ was therefore retained.

we obtain (Fig. 2*A*)

$$\overline{Z} = \overline{Z}_0 + \Delta Z(1 - \phi) \quad (A7)$$

From *Eq. A4*, we find

$$\frac{T' - \text{APD}}{T_0 - \text{APD}} = \frac{\alpha_4 - \alpha_4 g(\overline{Z}_0)}{\alpha_4 - \alpha_4 g(\overline{Z})} = \frac{\overline{Z} + k}{\overline{Z}_0 + k} \quad (A8)$$

Substituting for $\overline{Z}$ from *Eq. A7* into *Eq. A8* and solving for ΔZ, we find

$$\Delta Z = \left(\frac{T' - \text{APD}}{T_0 - \text{APD}} - 1\right)\left(\frac{\overline{Z}_0 + k}{1 - \phi}\right) \quad (A9)$$

Under control conditions, the influx of cations, ΔZ, that enter during the action potential must balance the ions removed by the electrogenic pump. Consequently, from *Eq. A2* we find

$$\gamma g(\overline{Z}_0) T_0 = \Delta Z \quad (A10)$$

Approximating $g(\overline{Z}_0)$ from *Eq. A3* and solving for γ, we obtain

$$\gamma = \frac{\Delta Z(\overline{Z}_0 + k)}{\overline{Z}_0 T_0} \quad (A11)$$

To summarize the procedure used to set the parameters, we first use *Eq. A4* to obtain α_4 from the experimentally measured duration of *phase 4* (at control), $t_4 = T_0 - \text{APD}$. *Equation A5* and the experimentally measured APD are then used to compute α_{APD} as a function of $\overline{Z}_0$. In the next step, by means of *Eq. A9*, we compute ΔZ from the perturbed cycle length after a premature action potential elicited at phase ϕ. Finally, using the steady-state condition, we calculate γ (12). Therefore the degree of postdrive prolongation and the rate of the subsequent decay to T_0 are controlled by a single parameter (T') determined from single-pulse experiments, which suggests that the kinetics of dissipation of overdive suppression are mainly governed by a steady-state condition for beat-to-beat variations in the level of Z (*Eq. A10*).

All the above parameters are a function of $\overline{Z}_0$. Because we have no direct way of measuring $\overline{Z}_0$ for each aggregate, we used the following method. A complete set of parameters was calculated for several values of $\overline{Z}_0$. For each value of $\overline{Z}_0$, the model was simulated to obtain a graph of overdrive supression at different frequencies of stimulation. The resulting family of curves was superimposed on the corresponding experimental data (Fig. 10). For $\overline{Z}_0 = 1.25k$–$1.75k$, there is good agreement between numerical simulation and experiment. Because qualitative aspects of overdrive suppression at different frequencies (in the 1:1 entrainment zone) are similar in all preparations (Fig. 7), an average value of $\overline{Z}_0 = 1.50k$ was assumed for all the experiments considered.

Finally, the amplitude of the stimulus employed in the numerical simulation was adjusted by matching the range of the 1:1 entrainment zone in the numerical simulation with the corresponding experimental results.

The values of the different parameters are summarized in Table 1.

The simple geometry of the limit cycle and the mode of action of the time-dependent component that affects y but not V (*Eq. 1*) is responsible for the lack of effect of the hyperpolarizing current on MDP in the numerical simulations. Indeed, such a hyperpolarization of MDP is sometimes observed during prolonged (> 1 min at 3 Hz) overdrive in spontaneously beating embryonic chick heart cell aggregates (20) and may contribute to the postdrive pause. Because of the short (typically < 30 s) duration of the drives used in our experimental protocols as well as the low value of membrane resistance at MDP, only a small effect of overdrive on MDP would be expected. This may explain the apparent lack of hyperpolarization of MDP observed in our overdrive protocols. In the context of the present theoretical model, such overdrive-induced changes in MDP could potentially be incorporated by letting the geometry of the limit cycle itself be influenced by increased action potential frequency. However, in view of the small magnitude of hyperpolarization observed in our experiments, such modifications are not warranted at the present time.

We thank Adam Sherman (Alembic Software) for computer software used in the experimental protocols and the analysis parts of this study.

Financial support was provided by the Quebec Heart and Stroke Foundation, the Natural Sciences Engineering Research Council, and the Fonds pour la Formation de Chercheurs et l'Aide à la Recherche.

Address for reprint requests: L. Glass, Dept. of Physiology, 3655 Drummond St., McGill University, Montreal, Quebec H3G 1Y6, Canada.

Received 7 March 1994; accepted in final form 30 March 1995.

REFERENCES

1. **Billette, J., R. Metayer, and M. St.-Vincent.** Selective functional characteristics of rate-induced fatigue in the rabbit atrioventricular node. *Circ. Res.* 62: 790–799, 1988.
2. **Carmeliet, E.** A fuzzy subsarcolemmal space for intracellular Na^+ in cardiac cells? *Cardiovasc. Res.* 26: 433–442, 1992.
3. **Cohen, J., H. Fozzard, and S. S. Sheu.** Increase in intracellular sodium ion activity during stimulation in mammalian cardiac muscle. *Circ. Res.* 50: 651–662, 1982.
4. **Courtney, K. R., and P. G. Sokolove.** Importance of electrogenic sodium pump in normal and overdriven sinoatrial pacemaker. *J. Mol. Cell. Cardiol.* 11: 787–794, 1979.
5. **DeHaan, R. L.** Regulation of spontaneous activity and growth of embryonic chick heart cells in tissue culture. *Dev. Biol.* 16: 216–249, 1967.
6. **FitzHugh, R.** Pulses and physiological states in theoretical models of nerve membrane. *Biophys. J.* 1: 445–466, 1961.
7. **Gadsby, D. C., J. Kimura, and A. Noma.** Voltage dependence of Na/K pump current in isolated heart cells. *Nature Lond.* 315: 63–65, 1985.
8. **Gilmour, R. F., J. R. Davis, and D. P. Zipes.** Overdrive suppression of conduction at the canine Purkinje-muscle junction. *Circulation* 76: 1388–1396, 1987.
9. **Glass, L., and M. Mackey.** *From Clocks to Chaos: The Rhythms of Life.* Princeton, NJ: Princeton University Press, 1988.
10. **Greenberg, Y. J., and M. Vassalle.** On the mechanism of suppression of automaticity in the guinea pig sinoatrial node. *J. Electrocardiol.* 23: 53–67, 1990.
11. **Guevara, M. R., L. Glass, and A. Shrier.** Phase locking, period-doubling bifurcations, and irregular dynamics in periodically stimulated cardiac cells. *Science Wash. DC* 214: 1350–1353, 1981.
12. **Guevara, M. R., L. Glass, and A. Shrier.** Phase resetting of spontaneously beating embryonic ventricular heart cell aggregates. *Am J. Physiol.* 251 (*Heart Circ. Physiol.* 20): H1298–H1305, 1986.
13. **Josephson, M. E.** *Clinical Cardiac Electrophysiology, Techniques and Interpretations* (2nd ed.). Philadelphia, PA: Lea & Febiger, 1993.
14. **Kowtha, V., A. Kunysz, J. R. Clay, L. Glass, and A. Shrier.** Ionic mechanisms and nonlinear dynamics of embryonic chick heart cell aggregates. *Prog. Biophys. Mol. Biol.* In press.
15. **Krellenstein, D. J., M. B. Pliam, C. M. Brooks, and M. Vassalle.** On the mechanism of idioventricular pacemaker suppression by fast drive. *Circ. Res.* 35: 923–934, 1974.

16. **Lederer, W. J., E. Niggli, and R. W. Hadley.** Sodium-calcium exchange in excitable cells: fuzzy space. *Science Wash. DC* 248: 283, 1990.
17. **Lieberman, M., C. R. Horres, J. F. Aiton, N. Shigetu, and D. M. Wheeler.** Developmental aspects of cardiac excitation: active transport. In: *Normal and Abnormal Conduction in the Heart: Biophysics, Physiology, Pharmacology, and Ultrastructure.* New York: Futura, 1982, p. 313–326.
18. **Meijler, F. L., and C. Fisch.** Does the atrioventricular node conduct? *Br. Heart J.* 61: 309–315, 1989.
19. **Musso, E., and M. Vassalle.** The role of calcium in overdrive suppression of canine cardiac Purkinje fibers. *Circ. Res.* 51: 167–180, 1982.
20. **Pelleg, A., S. Vogel, L. Belardinelli, and N. Sperelakis.** Overdrive suppression of automaticity in cultured chick myocardial cells. *Am. J. Physiol.* 238 (*Heart Circ. Physiol.* 7): H24–H30, 1980.
21. **Prinsze, F. J., and L. N. Bouman.** The cellular basis of intrinsic sinus node recovery time. *Cardiovasc. Res.* 25: 546–557, 1991.
22. **Talajic, M., D. Papadatos, C. Villemaire, L. Glass, and S. Nattel.** A unified model of AV node conduction explains dynamic changes in Wenckebach periodicity. *Circ. Res.* 68: 1280–1293, 1991.
23. **Van der Pol, B., and J. van der Mark.** The heartbeat considered as a relaxation oscillation, and an electrical model of the heart. *Arch. Neerl. Physiol.* 14: 418–443, 1929.
24. **Vassalle, M.** Electrogenic suppression of automaticity in sheep and dog Purkinje fibers. *Circ. Res.* 27: 361–377, 1970.
25. **Vassalle, M.** The relationship among cardiac pacemakers: overdrive suppression. *Circ. Res.* 41: 269–277, 1977.
26. **Vick, R. L.** Suppression of latent cardiac pacemaker: relation to slow diastolic depolarization. *Am. J. Physiol.* 217: 451–457, 1969.
27. **Vincenzi, F. F., and T. C. West.** Release of autonomic mediators in cardiac tissues by direct subthreshold electrical stimulation. *J. Pharmacol. Exp. Ther.* 141: 185–194, 1963.
28. **Wilders, R., H. J. Jongsma, and A. O. G. van Ginneken.** Pacemaker activity of the rabbit sinoatrial node. A comparison of mathematical models. *Biophys. J.* 60: 1202–1216, 1991.
29. **Winfree, A. T.** *The Geometry of Biological Time.* New York: Springer-Verlag, 1980.
30. **Zeng, W.-Z., L. Glass, and A. Shrier.** Evolution of rhythms during periodic stimulation of embryonic chick heart cell aggregates. *Circ. Res.* 69: 1022–1033, 1991.